Journal of Applied Polymer Science

Gradient and Weather Resistant Hybrid Super-Hydrophobic Coating Based on Fluorinated Epoxy Resin

Jin-Hua Li, Rui Weng, Xi-Qiang Di, Zeng-Wen Yao
Department of Material Sciences and Engineering, Wuhan University of Technology, Wuhan 430070, China
Correspondence to: J. -H. Li (E-mail: jinhua07@hotmail.com)

ABSTRACT: A weather resistant super-hydrophobic coating that can offer good substrate adhesion and yet to be easily processed at large scale can be of practical use in emerging fields of self-cleaning and anti-icing paint, combing all these properties together remains challenging task. Here we describe a composite coating composed of a fluorinated epoxy resin emulsion with embedded *in situ* surface-modified dual-scale nano-silica, which displayed durable super-hydrophobicity and excellent adhesive strength. The as-prepared coating possesses water contact angle of $158.6 \pm 1°$, sliding angle around $3.8 \pm 0.2°$ which remain stable even under acidic/alkaline, heat/cool, and accelerated aging treatment. The results demonstrate that surface roughness had a micron- and nanometer scale distribution with increased particle loading beyond 40 wt %. Through quantitative comparison of surface Attenuated Total Reflection (ATR) with bulk FT-IR transmission spectra, a gradient coating with surface enrichment of hydrophobic groups was determined. The air-side fluorinated polysiloxane-rich layer endows coating with weather-resistance and ultra-hydrophobicity while bottom epoxy resin layer enhances substrate adhesion. © 2014 Wiley Periodicals, Inc. J. Appl. Polym. Sci. **2014**, *131*, 40955.

KEYWORDS: coatings; functionalization of polymers; morphology; nanostructured polymers; surface and interface

Received 26 December 2013; accepted 4 May 2014
DOI: 10.1002/app.40955

INTRODUCTION

The remarkable water-repellent ability of lotus leaf provides biomimetic inspiration on constructing super-hydrophobic surface, which is commonly demonstrated with water contact angle (WCA) greater than 150° and sliding angle (SA) less than 10°.[1,2] It is well known that the particular lotus self-cleaning effect, owing to the surface unique geometrical structure and waxy materials, display promising potential in application fields of self-cleaning,[3] anti-icing,[4] oil-water separation,[5] and microfluidic channel.[6] As an effective approach, artificial roughness fabricating is often utilized to synergize the intrinsic hydrophobic surface and achieve extremely nonwettable surface.

Most previous attempts on mimicking lotus structure by various methods, such as plasma etching,[7] chemical vapor deposition,[8] microlithography, template technology,[9] phase separation,[10,11] and sol-gel,[12] depend on expensive equipment, complex procedures and bound to poor weatherability or production scale which show limitation in outdoor paint application. On the other hand, introducing nanoparticles into polymers [13] is common in large-area molding. Nanoparticles of photocatalytic TiO_2 have been blended with heptafluoro-poly (methylsiloxane) by Ding et al.[14] to obtain a long-term super-hydrophobic coating with decomposition ability of organic pollutants. Wang et al.[15] have combined nano-SiO_2 with chloroform dissolved hydrophobic polymethyl methacrylate, and the as-prepared coating also exhibited nice super water-repellence. However, a number of challenges still remain for practical use, despite some successful applications of this technique. Thin films of these materials tend to crack and peel off because of weak adhesion of matrix and poor resistance to diverse harsh environment. Hence, super-hydrophobic coating must further demonstrate stable weather-resistance, higher adhesive performance and large-area processability. Cross-linked epoxy resin, known for cost-effective, excellent mechanical strength, adhesion, and chemical stability, can be an ideal candidate, whereas the hydrophilic nature and poor weatherability are urgent to be improved. Moreover, *in situ* modification and emulsification on epoxy resin, instead of using organic solvent and complex post-hydrophobic treatment, may take account of both environmental painting and mass production feasibility simultaneously.

In the present work, we develop a novel approach to create weather-proof super-hydrophobic coating with enhanced WCA and low SA by embedding dual-scale silica into fluorinated epoxy emulsion system. The preparation of perfluorobutylsulfonyl polysiloxane, modification and emulsification on epoxy resin were required to form a gradient layer with bottom epoxy

Additional Supporting Information may be found in the online version of this article.

resin provide excellent adhesion and surface enriched hydrophobic groups. To better understand and optimize this superhydrophobic coating, further investigations on surface morphology, migration behavior of hydrophobic groups, weatherability, and thermal stability also have been conducted.

EXPERIMENTAL

Materials

Ethanol, toluene, triethylamine (TEA), and ammonia hydroxide (25wt %, C.P.) were all purchased from Sinopharm Chemical Reagent, Shanghai, China. 3-Aminopropyltriethoxysilane (APTES) was purchased from Wuhan University Silicone New Material, Hubei, China. Nanoscale silica (500, 100 nm) were supplied by Nanjing Haitai nano materials, China. Bis-aminopropyl polydimethylsiloxane (BAPS, average amino value of 2.6 mmol/g) was supplied by Dayi Chemical, Shandong, China. Perfluorobutylsulfonyl fluoride (PBSF) was provided by Wuhan Defu Economic Development, Hubei, China. Nonionic type self-emulsified waterborne epoxy curing agent (H208B) was purchased from Hanzhong Chemical, Shanghai, China, and E-44 epoxy resin (EP) was supplied by Baling Petrochemical, Hunan, China. All of them were utilized without any further treatment.

Synthesis

The intermediate of perfluorobutylsulfonyl bis-aminopropyl polydimethylsiloxane (PFBSBAPS) was prepared via typical sulfonyl amination reaction. With the existence of 0.12 mol TEA (acid capturer), about 0.1 mol PBSF was added dropwise into the mixture of 0.1 mol BAPS and 40 mL toluene under vigorous stirring at 50°C for 2 h. To remove excess TEA and salts, the resultant product was washed by saturated NaCl solution and vacuum dried for 24 h, a yellow viscous liquid was obtained. Certain amount of EP was then introduced to get a modified perfluorobutyl polysiloxane epoxy resin (PFBSEP). Finally, a target 50 wt % emulsion was prepared by blending the emulsifier H208B, PFBSEP and deionized water under vigorous stirring for 3 h.

Certain amount of nanoscale silica (combination of 500 and 100 nm with respective weight ratio of 1 : 2) was dispersed in aqueous ethanol and 10 wt % APTES was then added for 5 h reaction at 60°C to obtain amino functionalized nanoparticles. After mixed with fluorinated epoxy emulsion, a superhydrophobic film was constructed by dipping method on glass slides and curing at ambient atmosphere for 24 h.

Characterization

WCA measurement was carried out on contact angle tester (JC2000C, Shanghai Zhongchen Digital Technology Equipment. China). Typically, the results originated from average of five different droplets (about 4 μL/drop) across the surface. SA was measured by the same tester equipped with rotating accessory. The result was confirmed by average three measurements data with an accuracy of 0.2°. Surface topography was observed by SEM (JSM-5600LV, JEOL, Japan) and AFM (Multimode8, Veeco, USA), respectively. FT-IR (Nexus, Thermo Nicolet, USA) was used to determine structure of products and a KBr method was applied. Attenuated total reflection (ATR)-FTIR spectra were carried out to determine the surface enrichment of hydrophobic groups and Cary 630 FT-IR spectrometer (Agilent Technologies, USA) equipped with ATR accessory (Diamond ATR) was employed. The resolution was 2 cm^{-1} while 64 scans were set to obtain each spectrum and background was subtracted from all spectra. The weatherability of coating was tested under acid/alkali, heat/cool treatment and accelerated weathering process (UV aging chamber, ZP, Nanjing Testing Equipment, China). In addition, thermal analysis was conducted by simultaneous thermal analyzer (STA449c/3/G, NETZSCH Ltd., German with N_2 flow of 50 mL/min and heating rate of 10°C/min).

RESULTS AND DISCUSSION

Synthesis Mechanism of Fluorinated Epoxy Resin and FT-IR Characterization

The coupling agent APTES (about 10 wt % of the silica), through typical hydrolysis and condensation process, removed the ethyoxyl group and condensed with surface -OH of nanoparticle to realize functionalization. Actually, the excess APTES could inter-bond nanosilica to generate an aggregated silica microstructure.[16,17]

The synthesis of PFBSBAPS intermediate is mainly based on conventional aminolysis on acyl halide. As described in Figure 1 (step 1), the sulfuryl fluoride group of PBSF reacted with one terminal amino group of BAPS. Briefly, the outer most lone pair electrons on nitrogen-atom favors the nucleophilic attack on positive sulfonyl S atom and facilitated stripping F. In this reaction, the HF by-product was expected to be rapidly adsorbed by the dissolved acid capturer TEA. It noteworthy that although the reagents molar ratio and adding sequence are rigidly controlled, the existence of unreacted and complete fluorinated BAPS are inevitable. Figure 2 shows the FT-IR spectra, the stretching peaks of $–CH_3$, $-CH_2-$, -CH- appeared at 2962, 2905, 1412 cm^{-1} while the uniform peaks around 1020, 1261, 804 cm^{-1} in both spectra can be attributed to typical stretching vibration of -Si-O-Si-, in-plane bending and stretching vibration of $-Si-CH_3$ groups, respectively. In spectrum (b), comparing to BAPS, new absorption at 1604, 1352, 1209 cm^{-1} can be assigned to –NH, $-SO_2N-$, C-F bonds and also the weakening peak of $–NH_2$ at 3420 cm^{-1} demonstrate that the aminolysis reaction has occurred.

The fluorination of epoxy resin was simply carried out through nucleophilic addition reaction between $–NH_2$ of PFBSBAPS and epoxide groups as shown in Figure 1. It also should be noted that the final products contain both PFBSEP and other complex mixture because of the generated by-product from step 1. The emulsifier, as an epoxy modified polyamine, is not only waterborne but also a hydrotropy agent. Under vigorous shearing, this amphiphilic emulsifier enabled phase inversion to form PFBSEP latex particles with hydrophilic groups on the cover. Both amino groups on the cover of functionalized silica and latex particles have enabled the curing reaction to achieve crosslinked coating. The as-prepared emulsion has been diluted to different solid contents of 50, 35, and 20 wt % (Supporting Information Figure S1). They presented good stability until slight caking occurred after 3 days storage under room temperature. According to FT-IR spectra (Figure 3), the resultant

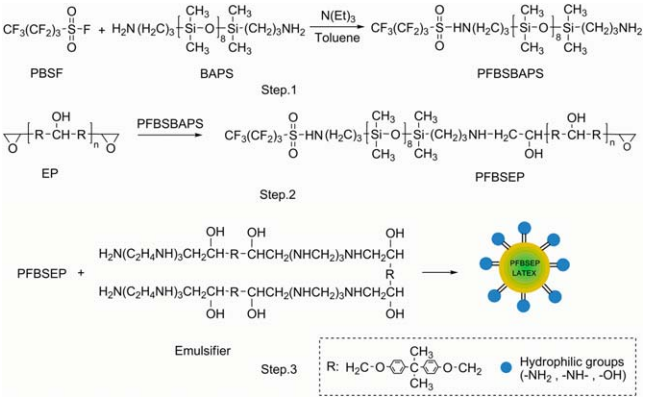

Figure 1. Three-step synthesis scheme of fluorinated epoxy emulsion. The PFBSBAPS is an ideally products, the resultant products should contain PFBSEP and other complex mixture of by-product. [Color figure can be viewed in the online issue, which is available at wileyonlinelibrary.com.]

coating spectrum showed new peaks at 3293, 1352, 802 cm^{-1} which associate with -NH-, $–SO_2N$- and Si-C formation. The widened absorption at 1190 cm^{-1} has further confirmed the existence of Si-O-Si bonds.

In addition, curing reaction of the PFBSEP coating with added emulsifier was also characterized by tracking the epoxide groups (914 cm^{-1}) in FT-IR spectra (see Supporting Information FigureS2). The internal standard of phenyl absorbance intensity at 1581 cm^{-1} was introduced and curing extent α was calculated by the following equation:

$$\alpha = 1 - (A_t/A_0)(A_{00}/A_{t0})$$

where A_0, A_{00} correspond to the epoxide group and phenyl absorbance intensity at the beginning of curing, respectively. A_t, A_{t0} represent the absorbance condition at certain time t during the curing process. It reveals that about 35% curing extent was achieved after 180 min drying at ambient atmosphere. Further drying for 24 h led to the disappearance of epoxide peaks, which indicates more complete reaction until approaching to 100% curing extent.

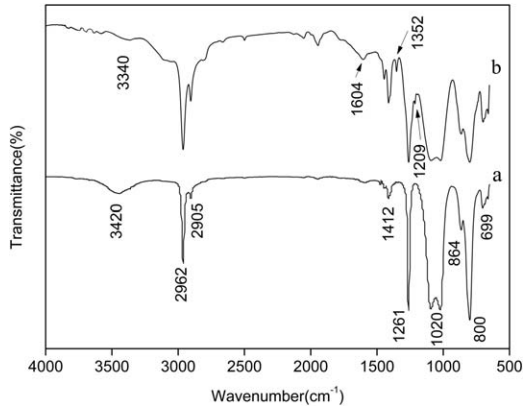

Figure 2. FT-IR spectrum of the reaction intermediates: (a) BAPS and (b) PFBSBAPS.

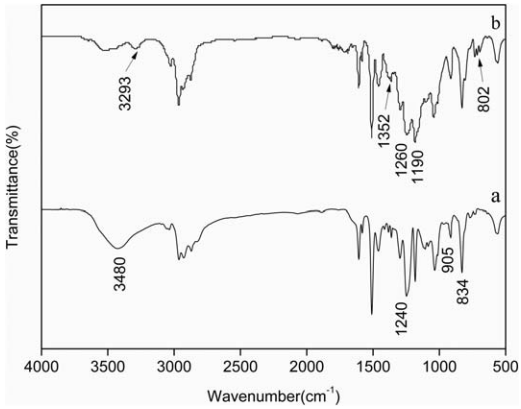

Figure 3. FT-IR spectrum of (a) E-44 epoxy resin and (b) PFBSEP.

Wettability Observation and Surface Morphology Evaluation

SEM was utilized to observe surface morphology. A typical smooth EP surface in Figure 4(a) just presents a hydrophilic WCA of $81.6 \pm 1°$. After fluorination, a hydrophobic coating with a larger WCA of $105.3 \pm 1°$, as depicted in Figure 4(b), was obtained but lots of white spots appeared on the surface. It represents fluorinated polysiloxane formed micro-domains, with which micro-phase separation occurred because of the dissimilarity of $–CF_x$, -Si-O- chains and epoxy resin main chain. A super water-repellent coating was observed, as depicted in Figure 4(c), by introducing 40 wt % of dual-scale silica into PFBSEP emulsion with WCA of $158.6 \pm 1°$, SA of $3.8 \pm 0.2°$. Obviously, water droplet was likely to stand on it. The SEM images describe numerous nano-scale silica with diameter around 100, 500 nm aggregated together to constitute irregular 3–4 μm protrusions at outmost layer. The only addition of nanosilica is previously reported[18] to generate micron/nanoscale roughness as well. In our experiment, 50 wt % addition of 100 nm nano-silica also enabled a super-hydrophobic coating formation with WCA of $157.5 \pm 1°$. However, the film was observed to be easily cracked during paint curing process and showed decreased substrate adhesion (Table II).

Generally, the relationship between surface roughness and wettability was investigated by the "sticky" Wenzel[19,20] and "slippery" Cassie-Baxter[21] models, which proposed the completely moistening and air-lifting theory of droplets on rough surface grooves, respectively. In order to clarify the effect of roughness on surface wettability, we have made a comparison of coating with different silica loadings. It can be seen in Figure 5, the contact angle was enhanced with increased nano-silica content, however, it was unable to go beyond 150° until 40 wt % nanoparticle was added. The AFM investigation illustrated a rising Root Mean Square (RMS) ranged from 159.7 to 299.0 nm while a narrow distribution of rough structures' height at 20 and 30 wt % transformed into a dual distribution with both micron and nanoscale size. An enhanced roughness factor r indicates the formation of micro-/nanoscale complex morphology, which provided higher specific surface area. It can be considered a wetting state transition has already existed. In brief, the less content of nano-silica just built mono-scale surface topography of Wenzel wetting, while 40 wt % addition was enough to construct hierarchical rough morphology with

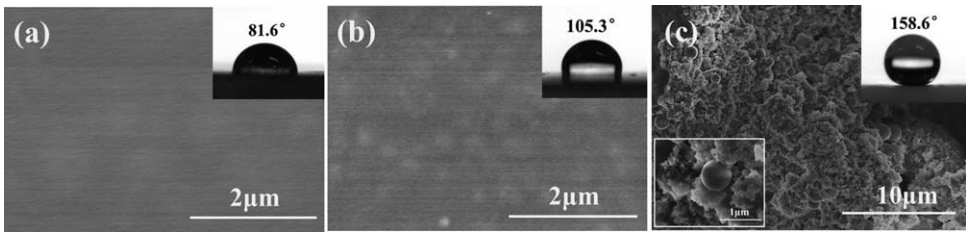

Figure 4. The surface SEM images of (a) original cured EP, (b) PFBSEP, and (c) super-hydrophobic coating (with partial magnification at left corner). The insets correspond to profiles of water droplets on each above surface, respectively.

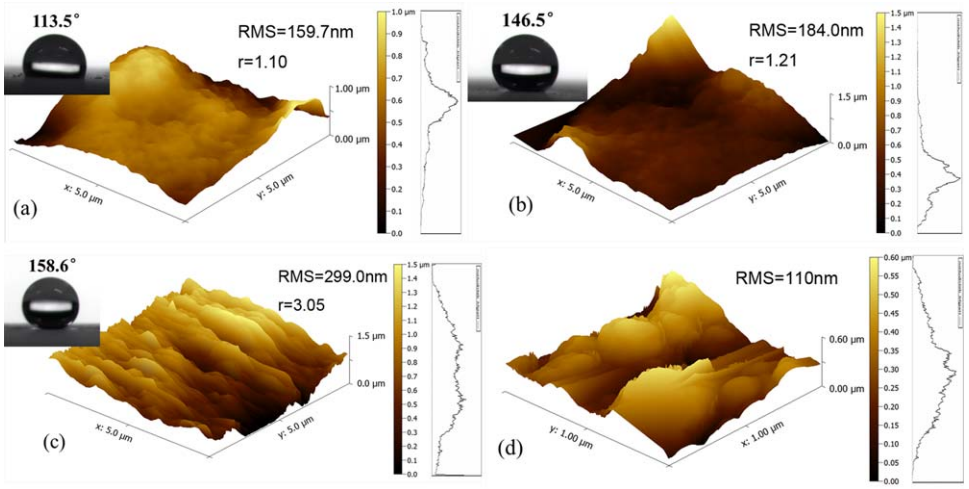

Figure 5. 3D AFM top-layer images contain RMS and r changes versus different silica loading at (a) 20 wt % (b) 30 wt %, (c) 40 wt %, respectively; and Image (d) indicates partial enlargement of (c). The right side spectrum corresponding to height distribution in each photo and the upper insets shows surface droplet contour. [Color figure can be viewed in the online issue, which is available at wileyonlinelibrary.com.]

sufficient air trapped in the gap to reach Cassie state. Dominate super-hydrophobic phenomena, the Cassie-Baxter equation stated as follows[22]:

$$\cos\theta^c = f_1\cos\theta_s - f_2$$

where θ^c and θ_s signify the apparent contact angle of droplets on rough surface and smooth surface, respectively. f_1, f_2 represent contact area fraction of solid–liquid and gas–liquid interface, respectively. With our experimental data of $\theta^c = 158.6°$, $\theta_s = 105.3°$, the result displayed as high as 90.6% of trapped air which lifted droplets to facilitate scrolling.

In addition, the typical Gibbs absorption formula was introduced to discuss hydrophobic groups' distribution:

$$\Gamma = -\frac{c}{RT}\cdot\frac{d\sigma}{dc}$$

In which, Γ, σ, and c represent the surface excess, surface tension and concentration, respectively. In terms of the fluoride polysiloxane surfactants, the surface energy of whole system would decrease while adding more surfactants, it means the $d\sigma/dc < 0$ and $\Gamma > 0$. It strongly implies the lowered surface energy can drive voluntarily mass migration of $-CF_x$ and -Si-O- chain onto the air side. Herein, ATR-FTIR (Supporting Information Figure S3) was employed to determine migration behavior of hydrophobic groups in the PFBSEP coating. Quantitative comparison of typical siloxane peaks (1010, 1085 cm^{-1}) in surface ATR spectrum with its bulk transmission data can offer estimation on the group distribution. As thickness and concentration often put great impact on absorbance intensity, we introduced the phenyl peak (1581 cm^{-1}) as an internal standard. The calculated results are listed in Table I. The A_{1010}, A_{1085}, and A_{1581} correspond to specific absorbance intensity, respectively, and ATR scan depth is 2 μm at 1700 cm^{-1}. The Si-O-Si concentration in surface layer is found nearly twice larger than the bulk concentration; it indicates a great air-side enrichment existed during coating formation. However, the quantitative analysis of $-CF_x$ was difficult to be conducted as these weak peaks were covered and hardly be observed. In spite of this, we can speculate the similar enrichment behavior also has occurred because of the much lower surface energy of fluorocarbon than siloxane chain.

Table I. Quantitative Analysis of ATR-FTIR and Transmittance FT-IR of PFBSEP Coating

	A_{1010}/A_{1581}	A_{1085}/A_{1581}
Bulk transmission	3.46	3.57
Surface ATR	8.82	6.74

Therefore, the fabrication mechanism of fluorinated epoxy resin based super-hydrophobic coating can be revealed in Figure 6.

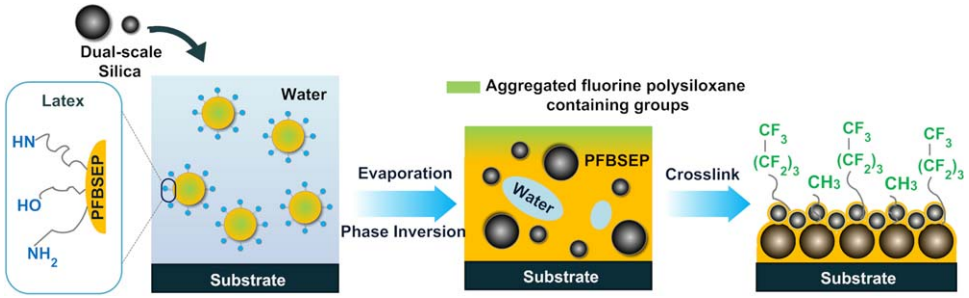

Figure 6. Illustration for the fabrication process of super-hydrophobic coating, include hydrophobic groups (green) self-assembling and emulsion film-forming process. [Color figure can be viewed in the online issue, which is available at wileyonlinelibrary.com.]

Nano-silica tends to aggregate together owing to the binding from coupling agent APTES and polymer matrix while low surface energy fluorinated polysiloxane migrates[23] to cover the surface rough structures. A gradient layer has formed with epoxy binder offer excellent adhesion and air-side fluorinated layer provided water-repellence. The synergy of hierarchical binary structure and hydrophobicity allowed the super-hydrophobic effect.

Weather Resistance Measurement and Thermal Analysis

More attractively, the super-hydrophobic coating, with 24 h curing, exhibited remarkable durability under both acidic/alkali, wide temperature range, and accelerated aging condition. As shown in Figure 7, slight WCA change of droplets with diverse pH value verifies the corrosion resistance and the 1 h heat/cooling treatment neither disturbed coating, which with large WCA remained greater than 150° from −10°C up to 90°C. Actually, the anti-corrosion can be ascribed to dense cross-linking chemical structure and shielding effect from fluorocarbon and siloxane-rich surface, which inhibited corrodent penetration and protected the reactive segment of backbone. Additionally, the image of Figure 8 illustrates a self-cleaning effect with extensive applicability, it worked not only on pure water but also on general fouls such as milk, tea, coffee, red wine, and ink. Accelerated weathering test was conducted to investigate the coating stability under UV irradiated damp-heat condition. The four-week aging brought only slight deterioration of WCA and SA (Figure 9). Actually, this fascinating weather-resistance can be owed to the surface enriched C-F and Si-O bonds, which possess high energy up to 485, 451 kJ/mol, respectively. They help immunize to UV irradiation (314–419 kJ/mol) and prevent EP main chain from the UV caused radical degradation and hydrolytic degradation of hydrophilic groups.

In thermal analysis, comparing to pure EP, the TG curves of super-hydrophobic coating in Figure 10 illustrates tiny change of $T_{d,5}$. The weight loss was mainly caused by removing adsorbed water and uncured reagents. Note that three separated peaks appeared in the differential thermal gravimetric (DTG) curves of coating, it may be ascribed to micro-phase separation in matrix and to some extent verifies our previous conclusion that incompatible chain segments existed. Briefly, the maximum weightless rate at 368.5°C represents degradation of EP main chain. The peak shift to 410.5°C may imply decomposition of the compatible chain segment, which derived from partly chemical bonding between epoxy resin and PFBSBAPS molecules. Meanwhile, degradation at 506.5°C owing to slight pyrolysis of linear polydimethylsiloxane chain, in which an unpaired electron of oxygen atom coordinated with adjacent empty 3d orbit

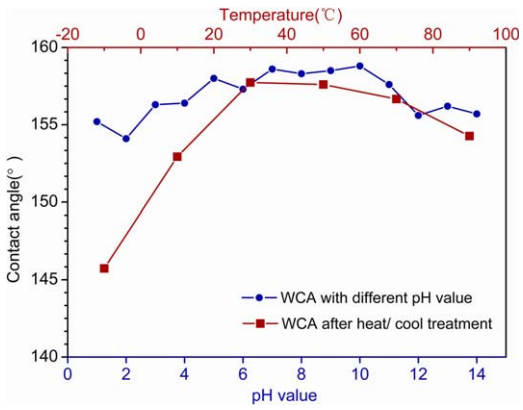

Figure 7. pH value and temperature influence on the contact angle of as-obtained self-cleaning coating. [Color figure can be viewed in the online issue, which is available at wileyonlinelibrary.com.]

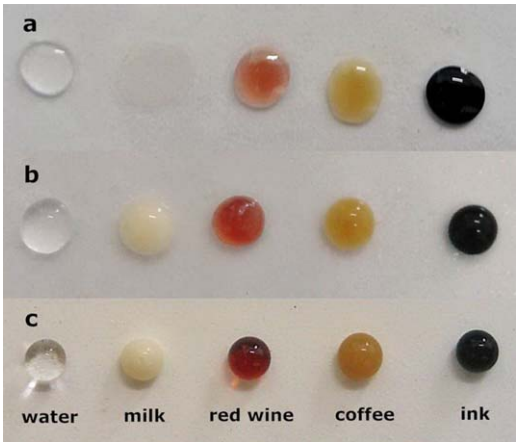

Figure 8. Photography of general foul liquids on (a) pure EP and (b) PFBSEP coating, and (c) super-hydrophobic film casted on glass substrates. [Color figure can be viewed in the online issue, which is available at wileyonlinelibrary.com.]

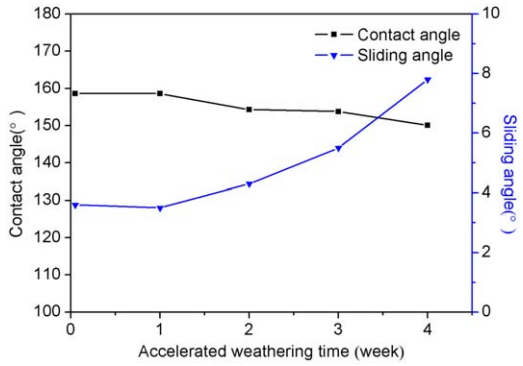

Figure 9. Contact angle and SA change of resultant coating during 4 weeks UV-accelerated aging process. [Color figure can be viewed in the online issue, which is available at wileyonlinelibrary.com.]

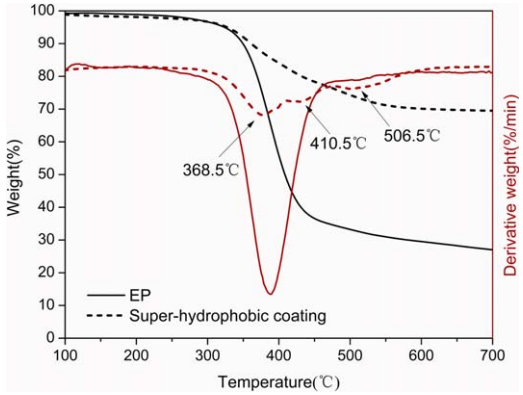

Figure 10. TG-DTG analysis of pure EP and super-hydrophobic coating under nitrogen atmosphere. The red lines correspond to DTG curves. [Color figure can be viewed in the online issue, which is available at wileyonlinelibrary.com.]

of Si to enable Si-O-Si breaking to form vaporizable cyclic siloxane.[24]

Furthermore, coating adhesion was tested via a peel-off method. A 10 mm × 10 mm surface area was divided into 100 squares and was peeled off by adhesive tape. The result originated from three different areas throughout surface. Prominent substrate (glass and aluminum) adhesion of super-hydrophobic coating with only 4% peeled off area can be found in Table II.

Table II. Coating Adhesion Properties Based on Peel-Off Method

Sample	Peeled off area	Adhesion level[a]
Pure EP	None	I
PFBSEP	None	I
20wt % SiO_2 coating	1%	I
30wt % SiO_2 coating	3%	I
40wt % SiO_2 coating	4%	I
50wt % 100 nm SiO_2 coating	10%	II

[a] The adhesion was divided into five levels. Level I was defined as peeled area ≤ 5%; Level II with 5–10% peeled area; Level III with 15–35% peeled area; Level IV with 35–65% peeled area; Peel-off area beyond 65% was considered as level V.

CONCLUSIONS

In summary, we report a feasible method to fabricate large-scale weather-resistant super-hydrophobic coating. By simply introducing dual-scale silica nanoparticles into ambient curable emulsion system of fluorinated epoxy resin, the coating displayed WCA of 158.6 ± 1° and SA around 3.8 ± 0.2°. The air-side enrichment of siloxane and fluorocarbon chains led to the formation of gradient layer. With excellent adhesive epoxy resin in bottom and strong $–CF_x$, -Si-O- bonds on the surface, our coating confers superior substrate adhesion and durability under various pH values, temperature range, and UV irradiated damp-heat condition. The obtained super water-repellence can be attributed to the synergy of matrix hydrophobic nature and the air-lifting effect of Cassie model, which existed in surface hierarchical geometry. We envision this weather-proof nonwettable coating to be highly useful in self-cleaning building, vehicle painting, drag-reduction microfluidic channel, and anti-ice coating of outdoor electric equipment.

ACKNOWLEDGMENTS

The authors wish to thank the experiment assistance from Peng Ding in state key laboratory of advanced technology for materials synthesis and processing and Yu-Bin Sun in materials research and testing center of Wuhan University of Technology.

REFERENCES

1. Yao, X.; Song, Y.; Jiang, L. *Adv. Mater.* **2011**, *23*, 719.
2. Yan, Y. Y.; Gao, N.; Barthlott, W. *Adv. Colloid Interface Sci.* **2011**, *169*, 80.
3. Chen, Z. J.; Guo, Y. B.; Fang, S. M. *Surf. Interface Anal.* **2010**, *42*, 1.
4. Cao, L. L.; Jones, A. K.; Sikka, V. K.; Wu, J. Z.; Gao, D. *Langmuir* **2009**, *25*, 12444.
5. Feng, L.; Zhang, Z. Y.; Mai, Z. H.; Ma, Y. M.; Liu, B. Q.; Jiang, L.; Zhu, D. B. *Angew. Chem. Int. Ed.* **2004**, *43*, 2012.
6. Mertaniemi, H.; Jokinen, V.; Sainiemi, L.; Franssila, S.; Marmur, A.; Ikkala, O.; Ras, R. H. A. *Adv. Mater.* **2011**, *23*, 2911.
7. Fresnais, J.; Benyahia, L.; Poncin-Epaillard, F. *Surf. Interface Anal.* **2006**, *38*, 144.
8. Borras, A.; Barranco, A.; Gonzalez-Elipe, A. R. *Langmuir* **2008**, *24*, 8021.
9. Berendsen, C. W. J.; Škereň, M.; Najdek, D.; Černý, F. *Appl. Surf. Sci.* **2009**, *255*, 9305.
10. Erbil, H. Y.; Demirel, A. L.; Avci, Y.; Mert, O. *Science* **2003**, *29*, 1377.
11. Aruna, S. T.; P. Binsy, E. Richard, Basu, B. *J. Appl. Surf. Sci.* **2012**, *258*, 3202.
12. Manca, M.; Cannavale, A.; Marco, L. D.; Arico, A. S.; Cingolani, R.; Gigli, G. *Langmuir.* **2009**, *25*, 6357.

13. Gao, N.; Yan, Y. Y.; Chen, X. Y.; Zheng, X. F. *J. Bionic. Eng.* **2010**, *7*, Suppl., S59.
14. Ding, X. F.; Zhou, S. X.; Gu, G.; Wu, L. M. *J. Mater. Chem.* **2011**, *21*, 6161.
15. Wang, J. Y.; Chen, X. H.; Kang, Y. K.; Yang, G. B.; Yu, L. G.; Zhang, P. Y. *Appl. Surf. Sci.* **2010**, *257*, 1473.
16. Xu, Q. F.; Wang, J. N.; Sanderson, K. D. *ACS Nano.* **2010**, *4*, 2201.
17. Westcott, S. L.; Oldenburg, S. J.; Lee, T. R.; Halas, N. J. *Langmuir* **1998**, *14*, 5396.
18. Yeh, K. Y.; Cho, K. H.; Chen, L. J. *Langmuir* **2009**, *25*, 14187.
19. Feng, L.;Zhang, Y. N.; Xi, J. M.; Zhu, Y.; Wang, N.; Xia, F.; Jiang, L. *Langmuir* **2008**, *24*, 4114.
20. Zheng, Y. M.; Bai, H.; Huang, Z. B.; Tian, X. L.; Nie, F. Q.; Zhao, Y.; Zhai, J.; Jiang, L. *Nature* **2010**, *463*, 640.
21. Zu, Y. Q.; Yan, Y. Y.; Li, J. Q.; Han, Z. W. *J. Bionic. Eng.* **2010**, *7*, 191.
22. Gao, X.; Jiang, L. *Nature* **2004**, *432*, 36.
23. Honda, K.; Morita, M.; Otsuka, H.; Takahara, A. *Macromolecules* **2005**, *38*, 5699.
24. Chen, H. P. *J. Am. Soc. Mass Spectrom.* **2003**, *14*, 1039.